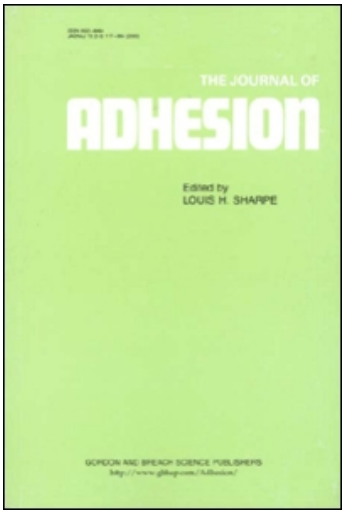

The Journal of Adhesion

Publication details, including instructions for authors and subscription information:
http://www.informaworld.com/smpp/title~content=t713453635

Theoretical Method to Predict the First Microcracks in a Scarf Joint

A. Objois[a]; J. Assih[a]; J. P. Troalen[a]
[a] Groupe de Mécanique, Matériaux et Structures (GMMS), Université de Reims Champagne-Ardenne, U.F.R Sciences/I.U.T, Reims Cedex 2, France

To cite this Article Objois, A. , Assih, J. and Troalen, J. P.(2005) 'Theoretical Method to Predict the First Microcracks in a Scarf Joint', The Journal of Adhesion, 81: 9, 893 — 909
To link to this Article: DOI: 10.1080/00218460500222819
URL: http://dx.doi.org/10.1080/00218460500222819

The Journal of Adhesion, 81:893–909, 2005

ISSN: 0021-8464 print/1545-5823 online
DOI: 10.1080/00218460500222819

Taylor & Francis
Taylor & Francis Group

Theoretical Method to Predict the First Microcracks in a Scarf Joint

A. Objois
J. Assih
J. P. Troalen
Groupe de Mécanique, Matériaux et Structures (GMMS),
Université de Reims Champagne-Ardenne, U.F.R Sciences/I.U.T,
Reims Cedex 2, France

In this work, we have calculated the theoretical threshold (F_d) of the first microcracks in the scarf joint. This threshold is particularly important because it marks the end of the elastic behavior of the bonded structure. At this point, the mechanical behavior of the adhesive is nonlinear and becomes dependent on the type of loading applied (dynamic tests, fatigue). Our method takes into account the geometrical variations of the joint as the scarf angle varies. We have used and adapted to our study a theoretical model based on the asymptotic-expansion method. The comparison between the theoretical values and the experimental thresholds determined by strain gauges and acoustic-emission techniques showed that the model accurately forecasts the microcracking of the joint provided that the scarf-angle value is more than 10°. When α is smaller than 10°, the theoretical model can no longer predict the very complex micromechanical behavior at the extremities of the joint, where the sharp ends of the adhesive layer and the metallic adherends coexist and react among themselves.

Keywords: Angular singularities; Bevel angle; Gradual damage; Microcracks; Micromechanical behavior; Scarf-joint bonded structure

INTRODUCTION

Among the different shapes of bonded structures, the scarf joint has been extensively studied and has been the subject of much experimental and theoretical research. This is mainly due to the high mechanical properties of this structure, regardless of the type of loading

Received 16 April 2004; in final form 7 March 2005.

Address correspondence to Anthony Objois, Groupe de Méchanique, Matériaux et Structures (GMMS), Université de Reims Champagne-Ardenne, Rue des Crayères, B.P. 1035, 51687 Reims Cedex 2, France. E-mail: anthony.objois@univ-reims.fr

applied. In fact, previous studies [1, 2] of the mechanical behavior of such an assembly in tension showed that the bevelled shape of the adherends enabled a notable reduction in the parasitic bending of the substrates because of the lack of alignment between the stresses in the joint and the direction of the applied load.

Our research has shown that for a bonded structure loaded in uniaxial tension, the adhesive damage is gradual and can be characterized, before the ultimate break, by two thresholds.

The first threshold, symbolized F_d, indicates the initiation of the first microcracks in a specific zone of the joint. The second threshold (denoted F_g) indicates the start of flaw propagation in an unsteady manner just before the ultimate break (denoted F_r).

Determination of the threshold of the first microcracks is fundamental because it marks the end of the elastic behavior of the bonded structure. F_d also corresponds to the level of reversibility beyond which the mechanical behavior of the joint is nonlinear and becomes dependent on the type of loading applied (dynamic tests, fatigue). The F_d threshold determination is especially important because, in some cases, these first microcracks in the adhesive can occur rapidly after the start of the tensile test for a level of loading less than the ultimate break. The experimental determination of the F_d threshold is a particularly long and expensive process that is not easy; this is why we have studied, in the scarf joint case, a method to predict F_d in a theoretical manner.

THEORETICAL METHOD PRINCIPLE

To forecast the F_d threshold value, we used and adapted to our study the theoretical analysis carried out by Wassiama [3], which is based on the asymptotic-expansion method of A. Rigolot adapted to bevelled joints. The main hindrance of this approach is the very complex micromechanical behavior of the various areas of the adhesive layer, especially near the bevelled extremities, where the microcracked zones coexist and react with the noncracked elastic zones. Indeed, our previous experimental works have shown, near the ends, the extent of the effects of the substrates' angular singularities on the micromechanical behavior of the adhesive layer. So, the microstrains measured on the adherends show that the zones of the joint where the first microcracks occurred do not match the zones where the theory forecasts the maximum stresses. Our method consists of an experimental study of the micromechanical behavior of the joint near the ends of the lap to precisely determine the zones of the joint where

the beginning of microcracking takes place and therefore where the stresses are maximized.

We then use the theoretical model to determine the external load corresponding to the ultimate strength of the adhesive in this precise area of the joint. This theoretical threshold of crack initiation is later compared with the experimental values determined with strain gauges on the specimens.

TEST SAMPLES

The specimen design is described in Figure 1. It is made up of two metallic bars bonded together with an adhesive joint.

The adherends are made of a ferritic steel with 0.18% carbon. The bars, with a 10 mm × 10 mm square cross section, are first machined by milling and finished with a grinding machine. To prevent the local plastic flow of the metallic sharp ends, especially for the low values of the angle α, the brittle bevelled ends are machined by electroerosion. Moreover, we use a special jig that allows accurate abutment of the substrates without spoiling the very sharp edge.

The adhesive is a two-component epoxy resin, "Eponal 317" (brand name of the French firm CECA); it polymerizes at room temperature (20 °C ± 1 °C) after mixing a resin (which contains mineral fillers) with a hardener.

The mechanical specifications of the adhesive are determined by using tensile tests carried out with standard specimens. The applied

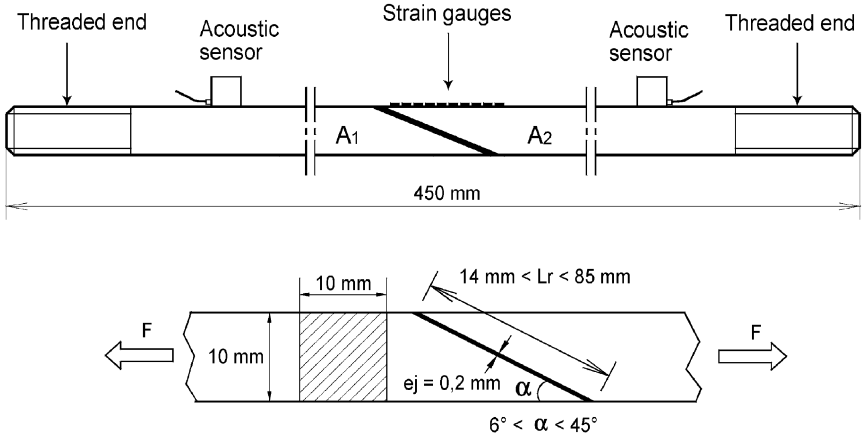

FIGURE 1 Scarf-joint bonded structure. Specification of the geometrical shapes and location of the acoustic cells and the strain gauges.

TABLE 1 Mechanical Properties of the Adherends and the Adhesive

Parameter	Steel	Adhesive
Young's modulus (MPa)	207700	5800
Poisson ratio	0.29	0.33
Breaking strength (MPa)	434	28.5

load *versus* microstrain relationship exhibits elastic/brittle behavior with a small viscoelastic component.

We made a set of three samples for each angle, α: 6°, 10°, 18°, 33°, and 45°. The length of the lap varies as a function of the angle, α, and so is equal to 85 mm, 56 mm, 32 mm, 18 mm, and 14 mm, respectively. The other parameters that affect the mechanical properties of the bonded structure, the adhesive thickness and the substrate roughness, were constant for all the specimens and near the optimal values determined in previous research [4, 5] (see Table 1). The adhesive layer was 0.2 mm thick and the surfaces where the adhesive was applied were sandblasted. This mechanical treatment gave to the surface a roughness equal to 11 μm, close to the average diameter of the mineral fillers (7 μm) contained in the adhesive. This roughness allows optimal adhesion between the substrates and the adhesive and so gives maximum strength to the joint. This last point is particularly important because the theoretical model was worked out on the assumption that the adhesion between the adhesive and the adherends was perfect [6].

The specimens are stressed in tension up to failure with a testing machine at a low loading rate ($200\,N \cdot s^{-1}$). The junction between the specimen and the machine is hinged to preserve the alignment between the longitudinal axis of the test sample and the direction of the applied load. This is very important because it avoids the premature cleavage failure of the bonded joint.

THEORETICAL ANALYSIS

For this work, we used and adapted the theoretical analysis carried out by Wassiama [3], which is based on the asymptotic-expansion method. We chose this model because it was capable of determining the stresses in the joint and in the adherends, taking into account the peculiar phenomena of stress concentration near the ends of the lap shown by experimental measurements. This difficulty has been partly resolved by using the "corrective method," which consists of

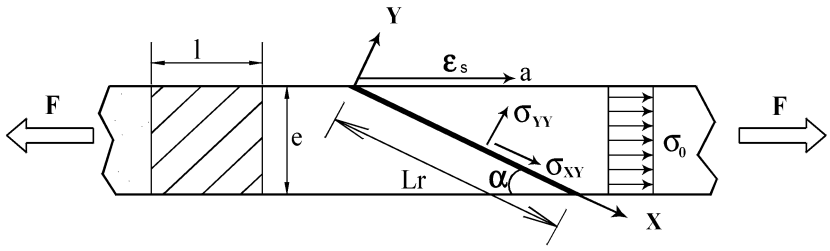

FIGURE 2 Theoretical model of scarf joint with boundary conditions: α, scarf angle; l, width of the adherends; e, thickness of the adherends; L_R length of the overlap; a, overlap abscissa; F, tensile load applied; E_S, Young modulus of the adherends; E_J, Young modulus of the adhesive; S, section of the sample; ν_S, Poisson's ratio of the adherends; ν_J, Poisson's ratio of the adhesive; σ_0, applied mean stress; σ_{XY}, shear stress in the joint; σ_{YY}, peel stress in the joint; ε_S, surface microstrain; χ, Airy function; and Π, Papkovitch's function.

adding a corrective stress field, having zero value in the central part of the overlap, and having significant values near the ends.

The theoretical equations were based on the following assumptions:

- The adhesive layer is sufficiently far from the ends of the specimen, where the tensile load, F, is applied, for the Saint-Venant assumption to be satisfied.
- On the crosssections of the substrates, the normal stress σ_0 (Figure 2) distribution is uniform.
- Taking into account the shape of the substrates, in particular their narrowness compared with their length, it is reasonable to make the plane-strain assumption.
- It is assumed that the low-carbon steel used for the adherends and the adhesive used for the joint are homogeneous and isotropic, and mechanical behavior is linear elastic.
- At the adhesive–substrate interfaces, where the strain field and the stresses field are continuous, the adhesion between the adhesive and the adherends is assumed to be perfect.

In the central part of the lap, far from the perturbed ends, shear stresses, σ_{XY}, and peel stresses, σ_{YY}, in the joint are obtained by the following equations [3]:

$$\begin{cases} \sigma_{XY} = \sigma_0 \sin\alpha \cos\alpha \\ \sigma_{YY} = \sigma_0 \sin^2\alpha \end{cases} \tag{1}$$

where $\sigma_0 = F/e \cdot l$.

Near the ends, the theoretical model of Wassiama [3] takes into account the end effect in adding corrective stresses to the previous relationships, given the following equations:

$$\begin{cases} \sigma_{XY} = \sigma_0 \sin\alpha \cos\alpha + \sigma_{XY}^{C}(X,Y) \\ \sigma_{YY} = \sigma_0 \sin^2\alpha + \sigma_{YY}^{C}(X,Y) \end{cases} \quad (2)$$

where σ_{XY}^{C} is corrective shear stress and σ_{YY}^{C} is corrective peel stress. These corrective stresses σ_{XY}^{C} and σ_{YY}^{C} are obtained by introducing an Airy function, χ.

$$\sigma_{XY}^{C} = \frac{-\partial^2\chi(X,Y)}{\partial y \partial x}, \quad \sigma_{YY}^{C} = \frac{\partial^2\chi(X,Y)}{\partial x^2}.$$

The Airy function $\chi(x,y)$ is calculated by the stationary functions method, where $\Pi(y)$ is the Papkovitch function, and stress decreases exponentially with distance from the ends of the lap:

$$\begin{aligned} \chi(x,y) &= e^{-2px}\Pi(y) \\ \Pi(y) &= A\cos[p(2y-1)] + B(2y-1)\sin[p(2y-1)] \end{aligned}.$$

The complex number, p, is the solution of the complex equation:

$$p - (3 + 4\nu_J)\sin p = 0$$

The constants A and B are related by the following equality:

$$A = B\frac{2(1-\nu_J) - (3+4\nu_J)\sin^2\frac{p}{2}}{p}$$

where $B = \left[-\frac{\nu_J}{1-\nu_J}\sin^2\alpha + \cos^2\alpha\right]\sigma_0 \Big/ 8p(2-Kp)$.

The Airy function $\chi(x,y)$ can be expressed by the following expression:

$$\chi(x,y) = 2Be^{-2px}\{K\cos[p(2y-1)] + (2y-1)\sin[p(2y-1)]\}$$

where

$$K = \frac{2(1-\nu_J) - (3+4\nu_J)\sin^2\left(\frac{p}{2}\right)}{p}$$

The K values *versus* p and Poisson's ratio, ν_J, of the adhesive are given in the Table 2.

TABLE 2 K Values *versus* p and Poisson's Ratio, ν_J, of the Adhesive

ν_J	0.25	0.30	0.35	0.40	0.45	0.50
p	2.475	2.503	2.529	2.553	2.576	2.595
K	−0.1155	−0.0889	−0.0611	−0.0321	−0.0025	−0.0280

The corrective stresses σ_{XY}^{C} et σ_{YY}^{C} are given by the expressions

$$\sigma_{XY}^{C} = \frac{\partial^2 \chi(x,y)}{\partial x \partial y}$$
$$= -8\mathrm{B}pe^{-2px}\{(1-Kp)\sin[p(2y-1)] - p(2y-1)\cos[p(2y-1)]\}$$
$$\sigma_{YY}^{C} = \frac{\partial^2 \chi(x,y)}{\partial x^2}$$
$$= 8\mathrm{B}p^2 e^{-2px}\{K\cos[p(2y-1)] + (2y-1)\sin[p(2y-1)]\}.$$

Figures 3 and 4 show the shear stress and the normal stress (peel stress) variation along the overlap for the different values of the angle α studied (6°, 10°, 18°, 33°, 45°). For convenience, the stress values σ_{XY} and σ_{YY} are expressed without units by making the ratio with the

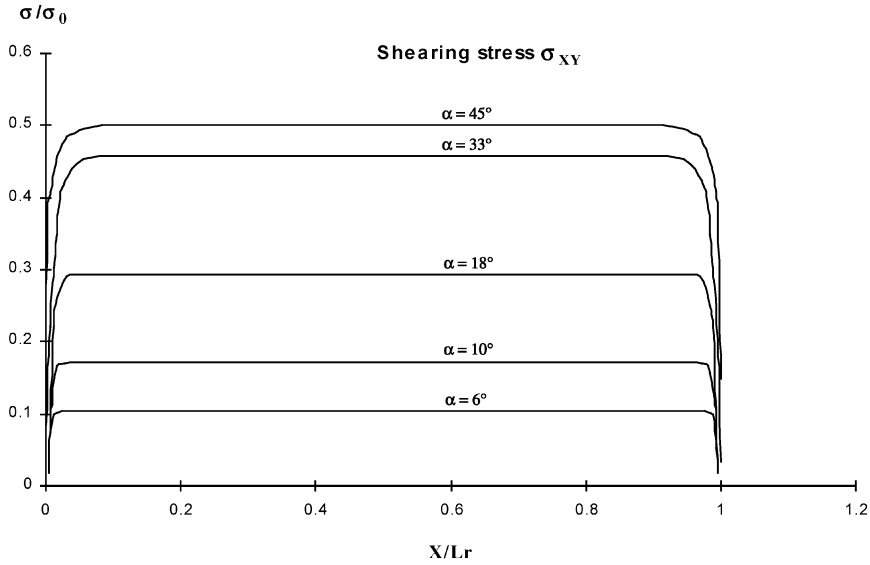

FIGURE 3 Variation of the normalized shear stress, σ_{XY}/σ_0, along the overlap for different values of the scarf angle (α) with σ_0 applied means stress in the adherends. The abscissa, X, of the joint is expressed *versus* the length of the overlap, L_R.

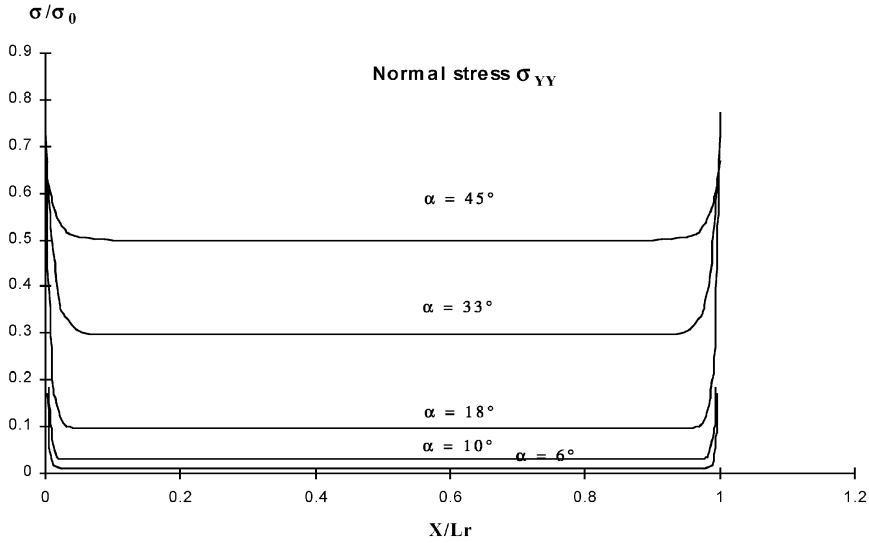

FIGURE 4 Variation of the normalized peel stress, σ_{YY}/σ_0, along the overlap for different values of the scarf angle (α) with σ_0 applied means stress in the adherends. The abscissa, X, of the joint is expressed *versus* the length of the overlap, L_R.

applied mean stress σ_0. Likewise, the abscissa X of the joint is expressed *versus* the length of the overlap L_R.

The figures show that the peel stresses and the shear stresses are uniform on a major part of the overlap, regardless of the value of the scarf angle. They also show a great variation in the stresses in the adhesive near the edges; indeed, the shear stresses decrease [7] quickly to become zero at the edge, whereas the peel stresses increase.

EXPERIMENTAL METHODS

The experimental method used to characterize the micromechanical behavior of the bonded joint was based on simultaneous measurements by strain gauges and acoustic-emission techniques during a tensile test [8].

The acoustic emission can be defined as a transient elastic wave generated by the rapid release of energy within a stressed material during its damage. If, as in our case, the specimen is made of a brittle adhesive and metallic adherends, each distinctive step of the damage of the joint can be detected by a significant increase in the acoustic emission. Indeed, when the applied load exceeds the elastic limit of

the adhesive, the successive relaxations of stresses resulting first from the initiation of microcracks and then from the propagation of flaws cause a sudden elastic-energy release and thus an increase in the acoustic activity.

The strain-gauge testing method is based on the analysis of variations of the surface microstrains. Thus, when microcracks start or when the propagation of cracks occurs in the adhesive joint, the microstrain field, measured along the outer surface of the adherends just above the damaged zone, is perturbed. Therefore, for each strain gauge, a change in the slope or a change in the sign of the curve $(dF/d\varepsilon)$ of the applied load *versus* the microstrain indicates initiation of microcracks or flaw propagation in the adhesive underneath this point.

It is worth noting, as shown in Figure 5, that both the acoustical method and the strain-gauge method gave similar results concerning the determination of the threshold (F_d) marking the initiation of

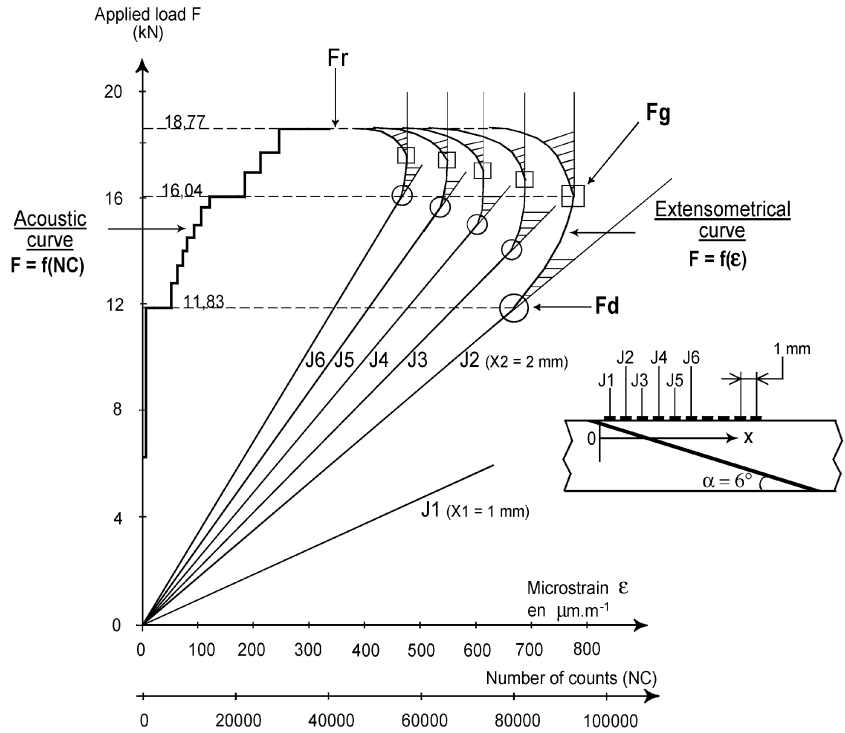

FIGURE 5 Correlation between the extensometric curve $F = f(\varepsilon)$ and the acoustic curve $F = f(NC)$. The adhesive layer is 0.2 mm thick and the angle α is equal to 6°.

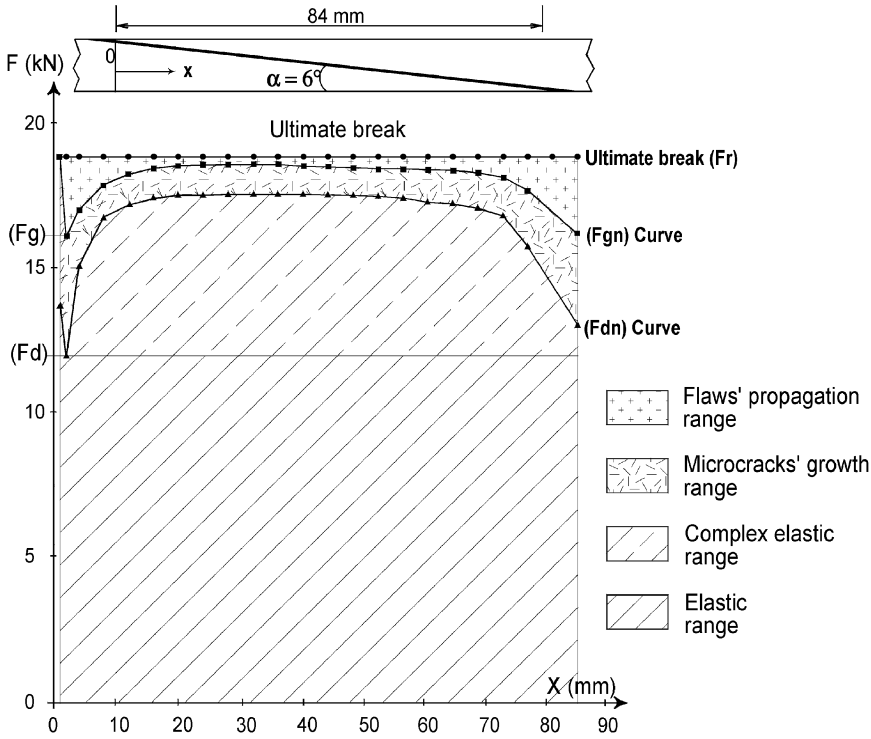

FIGURE 6 Representation of the various ranges of the micromechanical behavior of a scarf-joint bonded structure loaded in tension. Illustration of the case where $\alpha = 6^{\circ}$.

the first microcracks and the threshold (F_g) for the start of flaw propagation.

All of F_{d_n} and F_{g_n} values measured by the n gauges located along the lap make it possible to define different domains of the micromechanical behavior of the adhesive during its gradual damage (Figure 6):

- **The elastic domain** is constituted by the "global elastic range" defined by the interval $0 \leq F < F_d$ where neither zone of the joint is damaged, and the "complex elastic range" defined by the interval $F_d \leq F \leq F_{d_n}$ where the damaged zones adjoin the undamaged areas.
- **The growth range of the microcracks** is defined by the interval $F_{d_n} < F < F_{g_n}$ where microcracks are initiated in a steady manner in the adhesive.

- **The propagation range of the cracks** is defined by the interval $F_{g_n} \leq F < F_r$, where cracks propagated in an unsteady manner up to the final break.

These different domains are represented in Figure 6 which shows the gradual damage of a scarf-joint bonded structure loaded in tension in the case where the scarf-angle value is equal to 6°.

EXPERIMENTAL RESULTS

Tensile Tests and Experimental Arrangement

For each angle α studied, we have carried out three tension tests. Statistical analysis of the extensometric and acoustic results (Table 2) showed that the reproducibility of our test samples was satisfactory. Indeed, for each angle α studied, the standard deviations for the threshold for microcracks, the threshold for flaw propagation, and the threshold for ultimate failure were about 1%.

Influence of the Bevel Angle

The bevel angle substantially affects the micromechanical behavior of a scarf joint (see Figure 7). So, the mechanical strength of the joint, characterized by the thresholds F_d, F_g, and F_r, increases when the length of the overlap, L_R, increases. The values of the thresholds vary as a linear function of L_R up to 32 mm ($\alpha = 18°$) and, after that, when the value of L_R increases (α decreases), the mechanical strength of the joint increases more slowly. When the angle α is greater than 18°, the ultimate break occurs shortly after the first microcracks start and the cracks propagate. In this case, the bonded structure shows a significant "brittle character."

In contrast, it is remarkable that, when the angle α is less than 18°, the flaw propagation (threshold F_g) and the ultimate break (threshold F_r) occurs later, after the first microcracks (threshold F_d) start in the adhesive. We conclude that this better resistance of the joint to flaw propagation and the failure when L_R increases is due to the higher flexibility of thin adherends (in particular for the large length of the overlap). This higher flexibility allows a more uniform distribution of the stresses within the adherends and, thus, reduces the propagation of flaws in the joint. This feature gives a "plastic" behavior to the structure and therefore, makes the potential structural use of this bonded-joint design safer.

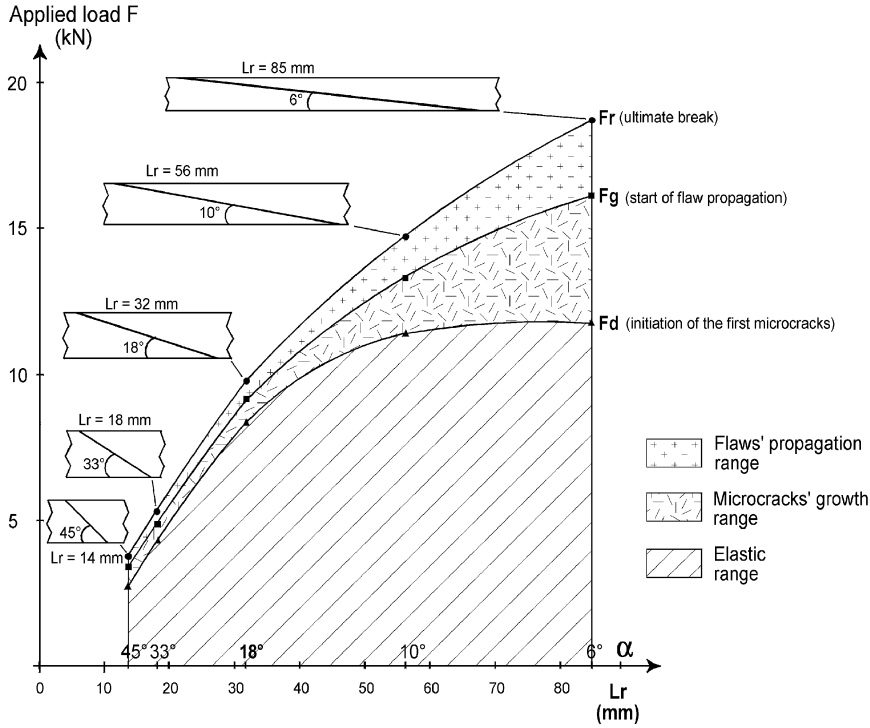

FIGURE 7 Influence of the bevel angle, α, and the length of the overlap (L_R) on the values of the damage thresholds F_d, F_g, F_r of the adhesive.

Micromechanical Behavior of the Joint near the Ends of the Lap

The experimental results show that the initiation of the first microcracks (threshold F_d) and the start of flaw propagation in unsteady manner (threshold F_g) do not take place exactly at the extremities (Figure 6) but in their neighborhood. After that, while the applied load increases, the microcracks extend step by step toward the middle of the overlap.

The initiation of the first microcracks does not occur at the extremities of the joint even though the stresses, in particular the peel stresses, are highest. We believe that this phenomenon can be explained by the local plastic flow of the metallic sharp ends, which makes the relaxation of stresses possible. This partial plastic flow is shown by the variations of the surface microstrains measured by electrical strain gauges J1 (Figure 7) located at the end of the overlap.

THEORETICAL PREDICTION OF THE FIRST MICROCRACK THRESHOLD

The principle of our method is to first calculate, with the theoretical model, the shear stress σ_{XY} and the peel stress σ_{YY} in the precise zone of the joint where the mechanical stress is highest. This zone is indirectly located by the strain gauge, which shows the maximum microstrain. After that, we used two boundary state criteria to combine the stresses σ_{XY} and σ_{YY} to characterize the stress state of the joint with a single stress ("equivalent stress"), symbolized σ_{EQ}. Next, we compare this single stress with the practical threshold of the initiation of the first microcracks corresponding to the rupture strength of the bulk adhesive (symbolized σ_R). In this way, we can determine what is the value of the external applied load that generates an equivalent stress, σ_{EQ}, equal to the rupture threshold, σ_R, of the adhesive.

We have calculated σ_{EQ} using the criterion of Von Mises and the criterion of St. Venant. Our choice is justified by their ease of use and the assumptions held in the theoretical analysis (plane strain, isotropic material, joint stressed in peeling and shearing). These two criteria are given by the following equations:

$$\text{Von Mises: } \sigma_{EQ} = \sqrt{3\sigma_{XY}^2 + \sigma_{YY}^2},$$

$$\text{St. Venant: } \quad \sigma_{EQ} = \frac{1-\nu_J}{2}\sigma_{YY} + \frac{1+\nu_J}{2}\sqrt{4\sigma_{XY}^2 + \sigma_{YY}^2}.$$

For this adhesive $\nu_J = 0.33$ and this last expression becomes

$$\sigma_{EQ} = 0.335\ \sigma_{YY} + 0.665\sqrt{4\sigma_{XY}^2 + \sigma_{YY}^2}.$$

To calculate the threshold of the first microcracks in the adhesive, the stress state must be determined in the most stressed zone of the joint. The theoretical model forecasts peak stresses in the ends of the overlap. Nevertheless, such stress concentration is not in accordance with physical reality. Indeed, we have shown in our experimental analysis that the sharp ends of the adherends adapt to these peak stresses. The experimental measurements by strain gauges show that the surface microstrains of the adherends are highest at a point located at a distance from the extremities that is closely related to the adhesive thickness. That is why the peel stresses and the shear stresses are calculated in the joint with the theoretical model, at a distance from the ends equal to the joint thickness.

TABLE 3 Threshold Values for the First Microcracks (F_d), the Propagation of Flaws (F_g), and for Ultimate Break (F_r), Determined by Strain-Gauge Testing and Acoustic Emission

Parameter	Specimen F_d	Angle or (deg) and length of overlap L_R				
		6° (85 mm)	10° (56 mm)	18° (32 mm)	33° (18 mm)	45° (14 mm)
F_d (kN)	1	11.83	11.34	8.32	4.23	2.84
	2	12.15	11.16	8.38	4.18	2.77
	3	11.92	11.19	8.41	4.27	2.88
F_g (kN)	1	16.04	13.22	9.29	4.90	3.38
	2	16.50	13.05	9.37	4.82	3.33
	3	16.32	13.16	9.40	4.95	3.43
F_r (kN)	1	18.77	14.59	9.76	5.18	3.66
	2	18.88	14.52	9.81	5.17	3.61
	3	18.55	14.44	9.85	5.21	3.68

After their combination in the equivalent stress criterion, the calculation with the model of the stresses σ_{XY} and σ_{YY} *versus* the applied mean stress makes the following expression possible: $_{EQ}$ $\sigma_{EQ} = k \cdot \sigma_0$.

The first microcracks take place in the joint when the rupture strength, σ_R, of the adhesive is reached, so when $\sigma_{EQ} = \sigma_R$, σ_R has been determined by tensile test to be 28.5 MPa.

σ_0 can be expressed *versus* the applied load, F, with the relationship $\sigma_0 = F/S$, where S is the section of the sample.

So, when the first microcracks occur in the adhesive, we have the equation $k \times (F_{d_T}/S) = 28.5$

where F_{d_T} is the theoretical threshold of the first microcrack initiation.

These theoretical values obtained by analytical calculation and the values F_d obtained by the experimental method are compared in Table 3 and in Figure 8.

Figure 8 shows that our theoretical method can be used to forecast with satisfactory accuracy the first initiation of the microcracks in an adhesive joint, provided that the scarf-angle value is more than 10°. In contrast, with very small angles (6° and less) of α, the theoretical values are not related to the experimental values. Indeed, the calculation forecasts a better resistance of the joint to microcrack initiation when α decreases even though the experimental measurements show that the microcrack strength of the joint no longer increases from $\alpha = 10°$.

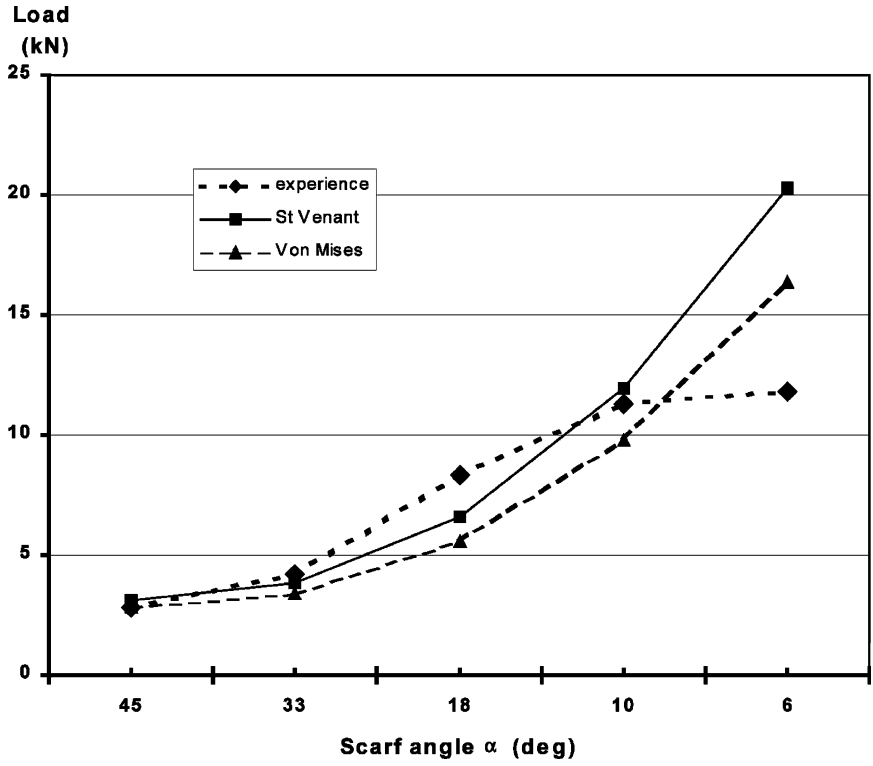

FIGURE 8 Comparison between the experimental and the theoretical values of the thresholds of the first microcrack initiation *versus* the length of the overlap.

CONCLUSION

The extensometric and acoustic methods give convergent results. In this way, they show that adhesive damage of bonded scarf joints starts a long time before the ultimate break. Thus, the threshold of the ultimate rupture of the bonded structure does not constitute a safe criterion. Our experimental measurements also show that the value of the scarf angle considerably affects the local and global mechanical properties of the bonded scarf-joint structure (Figure 7). When the length of the overlap increases (angle α decreases), the resistance of the joint to microcracks initiation (F_d), flaw propagation (F_g), and ultimate break (F_r) increases. These better mechanical properties can be partly explained by the more important surface of the overlap and also because the smaller the scarf angle, the more the adhesive layer is stressed in shearing. Furthermore, the greater flexibility of sharp ends

TABLE 4 Experimental and Theoretical Values of the Thresholds of the First Microcrack Initiation

	Angle or (deg) and length of overlap L_R				
F_d	6° (85 mm)	10° (56 mm)	18° (32 mm)	33° (18 mm)	45° (14 mm)
F_d experimental (kN)	11.83	11.34	8.32	4.23	2.84
F_{d_T} theorical, Von Mises (kN)	16.40	9.78	5.56	3.39	2.85
F_{d_T} theoricl, St. Venant (kN)	20.30	11.98	6.63	3.84	3.11

allows a better distribution of stresses in the adhesive and in the adherends, which gives the joint better resistance to microcrack growth and flaw propagation in an unsteady manner up to failure. This particular feature, which has been also observed in the case of a double-lap joint with scarfed ends of the outer adherends [9–11], is very interesting for industrial use. Indeed, with nondestructive techniques, it makes possible the detection of the threshold of, F_d, of the first microcrack initiation much before the ultimate break of the adhesive joint. Because knowledge of the F_d threshold of the bonded joints is, we believe essential, we have attempted to theoretically predict the F_d value.

Our results (Table 4) show that our theoretical method can predict the microcracking threshold of the adhesive when the scarf angle, α, is larger than 10°. When α was smaller than 10°, the theoretical values deviate from experimental values. Indeed, we can conclude that, in these borderline cases, the assumptions of the calculation are too restrictive. The theoretical model can no longer anticipate the very complex micromechanical behavior at the extremities of a joint, where the sharp ends of the adhesive layer and the metallic adherends coexist and react among themselves. Indeed, the sharp ends of a long overlap promote microcrack initiation in the adhesive by intensifying the local peak stresses in the joint. At the same time, they have a beneficial effect on the mechanical strength of the joint because the local plastic flow of the metallic sharp ends causes partial relaxation of stresses. Thus, although microcracked, the extremities of the joint adapt to the growing external load. So, Figure 7 shows that although the threshold of the first microcracks (F_d) was stabilized, when α was smaller than 10° the strength of the joint to the flaw propagation (F_g) and to the ultimate break (F_r) still increased. These results demonstrate the difficulty in predicting the micromechanical behavior of scarf joint, in particular for greater length of the lap. Indeed, the

micromechanical behavior of this scarf joint is so different between a short bevelled overlap and a long bevelled overlap that we consider them as two distinct joints. To make possible the theoretical prediction of the first microcrack threshold when the scarf angle α is very small, it is necessary to study the means to integrate, in the theoretical model, the specific action of the angular singularities of the sharp ends.

REFERENCES

[1] Lubkin, J. L., A theory of adhesif scarf joint, *J. Appl. Mech*. **255**, 255–260 (1957).
[2] Thein, W., Plane stress analysis of a scarf joint, *Int. J. Solids Structures* **12**, 491–500 (1976).
[3] Wassiama, A., Analyse théorique et expérimentale des contraintes dans un assemblage collé à simple recouvrement en biseau, Ph. D. dissertation, (1991).
[4] Mekiri, L., Contribution à líétude du comportement mécanique fin de líassemblage à simple recouvrement du type sifflet, sollicité en traction simple et en fatigue, Ph. D. dissertation, (1991).
[5] Objois, A., Gilibert, Y., and Fargette, B., Theoretical and experimental analysis of the scarf joint bonded structure: Influence of the adhesive thickness on the micro-mechanical behavior, *J. Adhes*. **70**, 13–32 (1999).
[6] Sancaktar, E., Recent approaches in constitutive behavior and testing of structural adhesives, *Appl. Mech. Rev*. **49**, 10, part 2, 128–138 (1996).
[7] Hart-Smith, L. J., Analysis and design of advanced bonded joints, *NASA CR2218* (1974).
[8] Stone, D. E. W. and Dingwall, P. F., Acoustic emission parameters and their interpretation, *NDT International* **10**, 51–62 (1957).
[9] Frigyes, T., Stress distribution in lap joints with partially thinned adherends, *J. Adhes*. **7**, 301–309 (1976).
[10] Ishal, O. and Gali, S., Two-dimensional interlaminar stress distribution within the adhesive layer of a symmetrical doubler model, *J. Adhes*. **8**, 301–312 (1977).
[11] Gilibert, Y. and Klein, M. L. L., Microcrack initiation in adhesive bonded double-lap joints with scarfed ends of outer adherends, *J. Adhes*. **28**, 51–69 (1989).